

Nonperturbative Renormalization in Strong Coupling QED₄

at the 8th Intern^l
Workshop on Light-Cone
QCD and Nonpert.
Hadronic Physics



(A.G. Williams,
CSSM, U. of Adelaide)

- Introduction
- The unrenormalized DSE's for QED₄
- The renormalized DSE's for QED₄
- Numerical results and multiplicative renormalization
- Conclusions and outlook

Based on work reported in:

F.T. Hawes and AGW, PRD 51, 3081 ('95)

F.T. Hawes, AGW, and C.D. Roberts, PRD 54, 5361 ('96)

F.T. Hawes, T. Sizer, and AGW, PRD 55, 3866 ('97)

A. Schreiber, T. Sizer, and AGW, in preparation.

with

F.T. Hawes (Florida State U.),
C.D. Roberts (Argonne Nat. Lab),

A. Schreiber (U of Adelaide)
T. Sizer (U of Adelaide)

Motivation:

"Try to do the best possible non-lattice treatment of strong-coupling quenched QED₄!"

"Non-lattice" + "Strong-coupling" \Rightarrow suggests, e.g., Dyson-Schwinger equations for detailed study

Approach:

\Rightarrow Try to do best possible DSE study of strong-coupling quenched QED₄.

QED is a good field theory to study with DSE's:

- Can use covariant gauge fixing and no Gribov copies to worry about (c.f., QCD).
- If proper photon-fermion vertex (Γ) is known, then coupled DSE's for photon propagator (D) and fermion propagator (S) are closed (i.e., fully determined).
- While complete Γ is not yet known, it is determined up to transverse parts by the Ward-Takahashi identity (WTI)

$$k_\mu \Gamma^\mu(p+k, p) = S^{-1}(p+k) - S^{-1}(p).$$

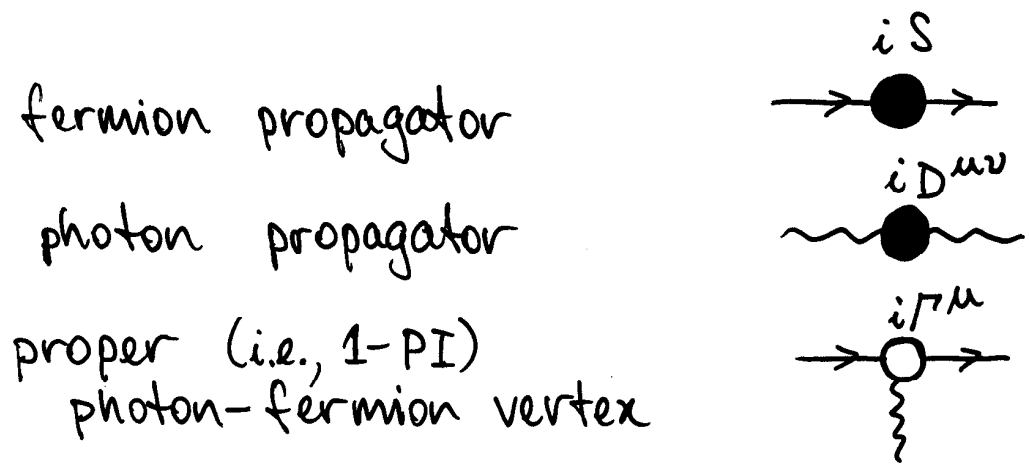
In addition Γ must have:

- correct CPT transformⁿ properties
- no artificial kinematic singularities
- perturbative form in weak-coupling limit
- correct behavior to ensure appropriate gauge covariance of DSE's

Interesting recent developments:

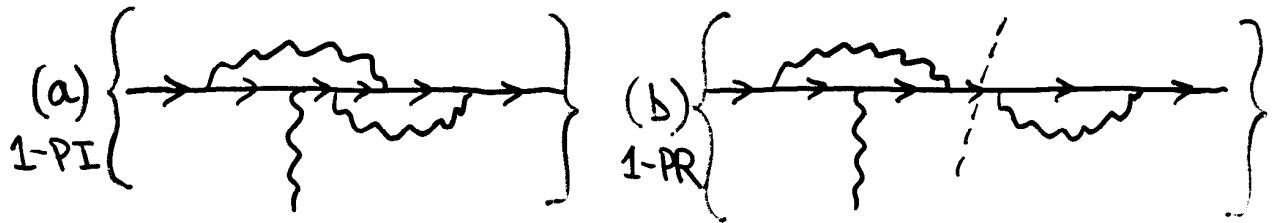
- Exploit Landau-Khalatnikov gauge transformⁿ properties of S !
- Kondo has recently argued that transverse vertex is almost completely specified in chiral limit in QED₂. Extension to QED₄ ???
- Bashir, Kizilersu, + Pennington have improved ansatz for transverse vertex, (consistent with MR etc.)

Graphical representation:



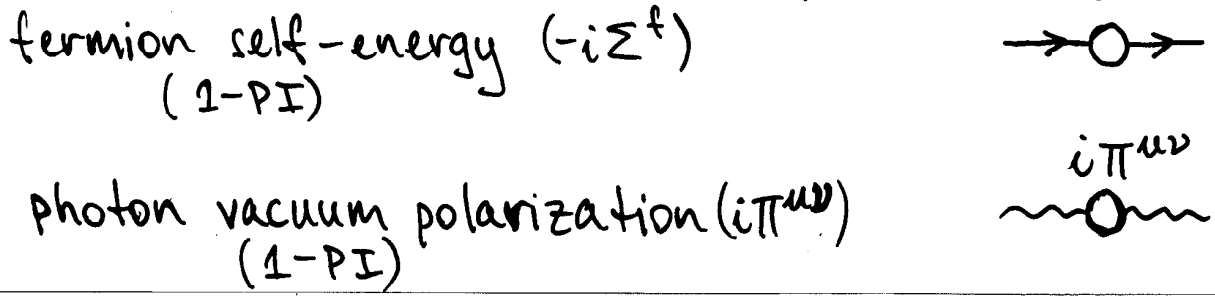
$\left\{ \begin{array}{l} \text{filled} \\ \text{unfilled} \end{array} \right\}$ circles \Leftrightarrow $\left\{ \begin{array}{l} \text{connected} \\ \text{proper (i.e., 1-PI)} \end{array} \right\}$ Green's functions
 \Leftrightarrow sum of all $\left\{ \begin{array}{l} \text{connected} \\ \text{proper (i.e., 1-PI)} \end{array} \right\}$ Feynman diagrams

Defⁿ: Proper or 1-PI Feynman diagrams do not become disconnected when one internal line is cut.



So (a) contributes to the proper vertex but (b) does not.

Hence can also define for example:



Dyson-Schwinger Equation (DSE) for the Photon Propagator:

It is easiest to see these using sums of Feynman diagrams, (but note can also derive directly from functional integral.)

a) $i\Pi = i\Gamma + i\gamma$

b) $iD = iD_0 + iD_0 i\Pi iD$

$$\begin{aligned}
 i\Pi &= \text{[diagram 1]} + \text{[diagram 2]} + \text{[diagram 3]} \\
 &\quad + \text{[diagram 4]} + \text{[diagram 5]} + \dots \\
 &= \text{[diagram 6]} + \text{[diagram 7]} + \text{[diagram 8]} \\
 &\quad + \text{[diagram 9]} + \text{[diagram 10]} + \dots \\
 &= \text{[diagram 11]}
 \end{aligned}$$

every Feynman diagram is contained once and only once on LHS and RHS of (a)

Can write then by inspection ↗

$$\textcircled{*} \left[i\Pi^{\mu\nu}(k) = (-1) \sum_f (e_f^t)^2 \int \frac{d^d l}{(2\pi)^d} \text{tr} \left[(i\gamma^\mu)(iS^t)(i\not{k}\not{l}) (iS^t) \right] \right]$$

$$\begin{aligned}
 iD &= iD_0 + \text{[diagram: loop with self-energy]} + \text{[diagram: loop with vacuum polarization]} \\
 &+ \text{[diagram: loop with self-energy and vacuum polarization]} + \text{[diagram: loop with vacuum polarization and self-energy]} + \dots \\
 &+ \text{[diagram: two loops]} + \text{[diagram: two loops with vacuum polarization]} + \dots \\
 &= iD_0 + iD_0 i\pi iD
 \end{aligned}$$

[Needs thought but again 1-to-1 correspondence for LHS and RHS]

Gauge invariance in QED \Rightarrow set of identities called Ward-Takahashi identities (WTI).

One such identity is

$$* \boxed{k_\mu \pi^{\mu\nu} = 0} *$$

\Rightarrow Define $\pi(k^2)$ by then since

$$\pi^{\mu\nu}(k) \equiv (-g^{\mu\nu}k^2 + k^\mu k^\nu) \pi(k^2)$$

$$* \left[D_0^{\mu\nu}(k) \equiv (\text{free photon propagator}) = \frac{-g^{\mu\nu} + \frac{k^\mu k^\nu}{k^2}}{k^2} - \int_0^1 \frac{k^\mu k^\nu}{k^4} \right]$$

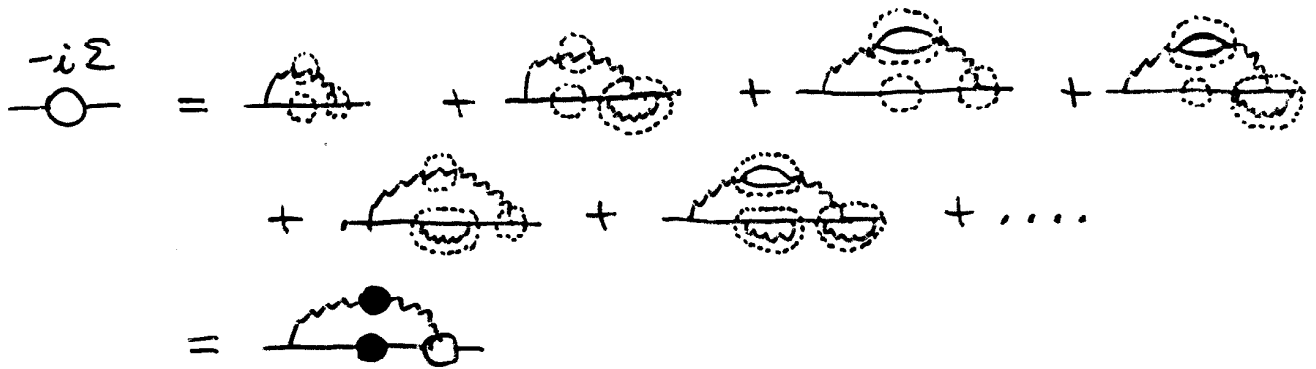
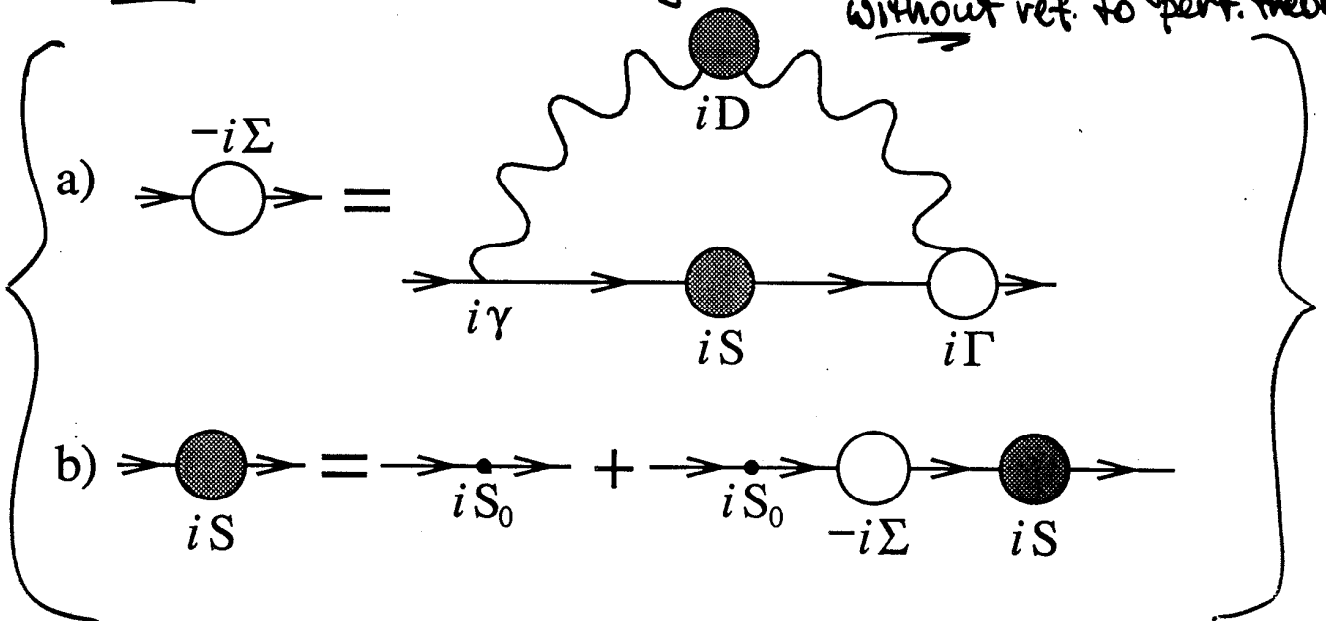
we can invert $iD^{\mu\nu} = iD_0^{\mu\nu} + iD_0^{\mu\sigma} i\pi_{\sigma\tau} iD^{\tau\nu}$ to write

$$* \left[D^{\mu\nu}(k) \equiv (\text{photon propagator}) = \left(\frac{-g^{\mu\nu} + \frac{k^\mu k^\nu}{k^2}}{k^2} \right) \frac{1}{1 + \pi(k^2)} - \int_0^1 \frac{k^\mu k^\nu}{k^2} \right]$$

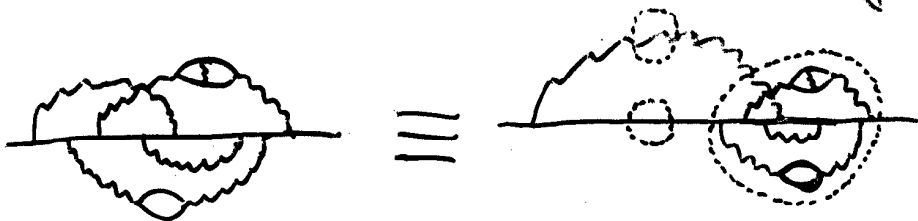
DSE for the Fermion Propagator:

Again, every Feynman diagram contributing to LHS appears once and only once on RHS.

(Note: Can also derive directly from functional integral without ref. to pert. theory)



Sometimes it helps to redraw a Feynman diagram eq.



$$\textcircled{*} \left[-i \Sigma^f(p) = (e_0^f)^2 \int \frac{d^d \ell}{(2\pi)^d} (i\gamma^\mu) (iS^f) (iD_{\mu\nu}) (i\Gamma^{\nu}) \right]$$

Can write by inspection using usual Feynman-type rules.

$$\begin{aligned}
 \begin{array}{c} iS \\ \rightarrow \bullet \rightarrow \end{array} &= \begin{array}{c} iS_0 \\ \rightarrow \bullet \rightarrow \end{array} + \begin{array}{c} \text{---} \text{---} \text{---} \\ \text{---} \text{---} \text{---} \end{array} + \begin{array}{c} \text{---} \text{---} \text{---} \\ \text{---} \text{---} \text{---} \end{array} \\
 &+ \begin{array}{c} \text{---} \text{---} \text{---} \\ \text{---} \text{---} \text{---} \end{array} + \dots \\
 &= \begin{array}{c} iS_0 \\ \rightarrow \bullet \rightarrow \end{array} + \begin{array}{c} iS_0 \quad iS \\ \rightarrow \circ \rightarrow \bullet \rightarrow \\ -i\Sigma \end{array}
 \end{aligned}$$

Again 1-to-1 correspondence between LHS and RHS

Can use

$$\textcircled{*} \left[S_0^f(p) = \frac{1}{\not{p} - m_0^f} \right]$$

and invert $iS^f = iS_0^f + iS_0^f (-i\Sigma^f) iS^f$
to give

$$\textcircled{*} \left[S^f(p) = \frac{1}{\not{p} - m_0^f - \Sigma^f(p)} \right]$$

proof:

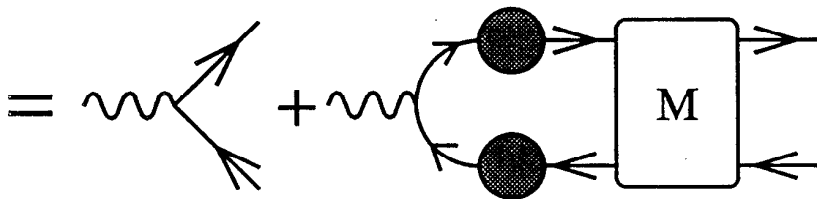
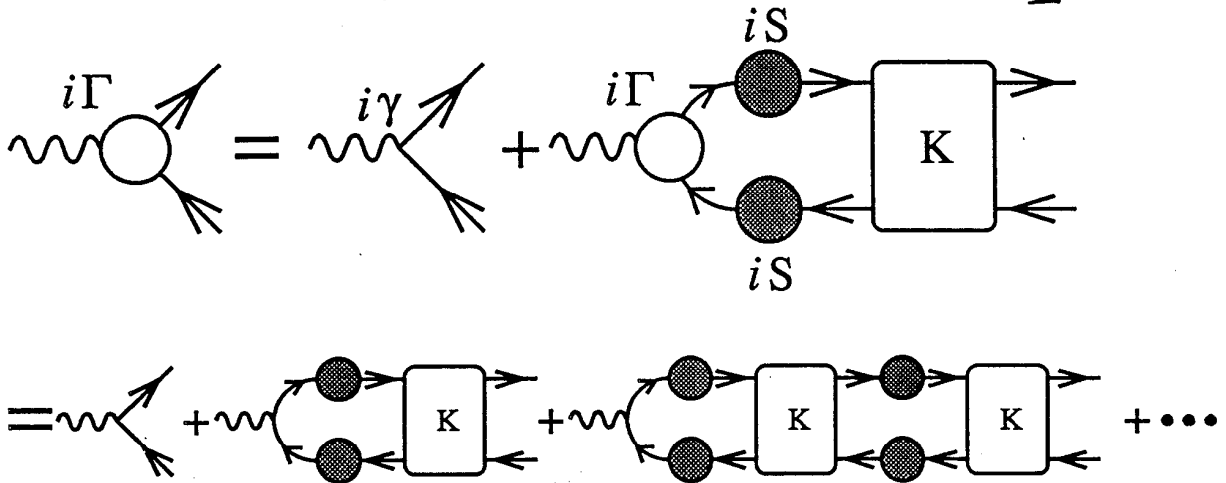
$$\begin{aligned}
 iS^f(p) &= iS_0^f(p) + iS_0^f(p) (-i\Sigma^f(p)) iS^f(p) \\
 \Rightarrow S^f &= S_0^f + S_0^f \Sigma^f S^f \\
 \text{now act on LHS with } (S_0^f)^{-1} \text{ and RHS with } (S^f)^{-1} \\
 \Rightarrow (S_0^f)^{-1} &= (S^f)^{-1} + \Sigma^f \\
 \Rightarrow (S^f)^{-1} &= (S_0^f)^{-1} - \Sigma^f = \not{p} - m_0^f - \Sigma^f \\
 \Rightarrow S^f(p) &= \frac{1}{\not{p} - m_0^f - \Sigma^f(p)}
 \end{aligned}$$

There is a **WTI** relating the fermion propagator and the photon-fermion proper vertex

$$\textcircled{*} \quad i k_\mu \Gamma^{f\mu}(p+k, p) = (S^f)^{-1}(p+k) - (S^f)^{-1}(p)$$

DSE for Fermion-Photon Proper Vertex:

$$\textcircled{*} \left[i\Gamma_{\mu}^f(p', p) = i\gamma_{\mu} + \sum_{g=1}^{N_f} \int \frac{d^d \ell}{(2\pi)^d} (iS^g) (i\Gamma_{\mu}^g) (iS^g) K^{gf} \right]$$



$K \equiv$ (fermion-antifermion scattering kernel)

$$= \text{[tree-level kernel]} + \text{[loop kernel]} + \text{[tree-level kernel]} + \text{[loop kernel]} + \dots$$

kernel "K" is 2-PI with respect to fermion anti-fermion pair,

whereas $M = K + K(iS)^2 K + K(iS)^2 K(iS)^2 K + \dots$ is not.

Renormalized DSE's in QED

To renormalize QED some intermediate regularization is understood. Then define

$$\psi_0^f \equiv \sqrt{z_2^f} \psi^f \quad A_0^\mu \equiv \sqrt{z_3} A^\mu \quad e_0^f \equiv \frac{z_1^f}{z_2^f \sqrt{z_3}} e^f$$

and the renormalized action \tilde{S}_f by

$$\tilde{S}_f[\bar{\Psi}, \Psi, A^\mu] \equiv S_f[\bar{\Psi}_0, \Psi_0, A_0^\mu]$$

$$\Rightarrow \tilde{S}_f[\bar{\Psi}, \Psi, A^\mu] = \int d^d x \left[\sum_f \left\{ z_2^f \bar{\Psi}^f (i\not{\partial} - m_0^f) \Psi^f + z_1^f e^f \bar{\Psi}^f \not{A} \Psi^f \right\} - \frac{z_3}{4} F_{\mu\nu} F^{\mu\nu} - \frac{z_3}{2\xi_0} (\partial_\mu A^\mu)^2 \right]$$

$$= \int d^d x \left[\sum_f \left\{ \bar{\Psi}^f (i\not{\partial} - m^f + e^f \not{A}) \Psi^f - \frac{1}{4} F_{\mu\nu} F^{\mu\nu} \right. \right.$$

$$\left. - \frac{1}{2\xi} (\partial_\mu A^\mu)^2 \right\} + \sum_f \left\{ (z_2^f - 1) \bar{\Psi}^f i\not{\partial} \Psi^f - \delta m^f \bar{\Psi}^f \Psi^f \right\} \\ \left. + \delta e^f \bar{\Psi}^f \not{A} \Psi^f - \frac{(z_3 - 1)}{4} F_{\mu\nu} F^{\mu\nu} \right]$$

"counterterms"

where $\xi_0 \equiv z_3 \xi$, $\delta m^f = z_2^f m_0^f - m^f$, $\delta e^f = (z_1^f - 1) e^f$.

Terms in red are "counterterms".

e^f, m^f, ξ \equiv renormalized quantities

Procedure: Use "blue" expression for \tilde{S}_f and define as before (by analogy) \tilde{Z}, \tilde{G} , and $\tilde{\Gamma}$.

Then define $\tilde{D}^{-1} \equiv \frac{\delta^2 \tilde{\Gamma}}{\delta A \delta A} \Big|_{\bar{\Psi}=\Psi=A=0}$, $\tilde{S}^{-1} \equiv \frac{\delta^2 \tilde{\Gamma}}{\delta \bar{\Psi} \delta \Psi} \Big|_{\bar{\Psi}=\Psi=A=0}$
etc.

Renormalized quantities:

$$\left[\begin{aligned} \tilde{D}^{\mu\nu}(k) &\equiv \left[\frac{-g^{\mu\nu} + k^\mu k^\nu / k^2}{k^2} \right] \frac{1}{1 + \tilde{\Pi}(k^2)} - \xi \frac{k^\mu k^\nu}{k^4} \\ \tilde{S}^f(p) &\equiv \frac{1}{\not{p} - m^f - \tilde{\Sigma}(k)} \\ \tilde{\Gamma}^{f\mu}(p', p) &= \gamma^\mu + \tilde{\Lambda}^{f\mu}(p', p) \end{aligned} \right]$$

where, e.g., the renormalized self-energies are

$$\tilde{\Pi}(q^2) = \Pi'(q^2) + (Z_3 - 1)$$

where

$$i\Pi'_{\mu\nu} = (-1) \sum_f Z_1^f (e^f)^2 \int \frac{d^d l}{(2\pi)^d} \text{tr}[\gamma_\mu \tilde{S}^f \tilde{\Gamma}_\nu^f \tilde{S}^f]$$

$$\tilde{\Sigma}(p) = \Sigma'^f(p) - (Z_2^f - 1)\not{p} + (Z_2^f m_0^f - m_f)$$

where

$$-i\Sigma'^f(p) = Z_1^f (e^f)^2 \int \frac{d^d l}{(2\pi)^d} \gamma^\mu \tilde{S}^f \tilde{D}_{\mu\nu} \tilde{\Gamma}^{f\nu}$$

etc.

Last step in renormalization program is to set the renormalization point μ and impose the B.C.'s, (i.e., choose $m^f(\mu)$, $\alpha(\mu)$, and $\xi(\mu)$)

$$\Rightarrow \tilde{\Sigma}(p) \Big|_{p^2=\mu^2} = 0, \quad \tilde{\Pi}(k^2) \Big|_{k^2=0} = 0,$$

$$\tilde{\Gamma}^f(p', p) \Big|_{p'^2=p^2=\mu^2} = \gamma^\mu + (\text{other terms})$$

$$\Rightarrow Z_1^f, Z_2^f, Z_3, m_0^f \text{ determined } (Z_1^f = Z_2^f)$$

and
 ★ Note: e^f and m^f are physical charge and mass }
 only for on-shell renormalization, i.e., μ is pole in \tilde{S}^f }

Further notes on the renormalized theory:

→ Recall that since the renormalized theory replaces the action S_0 by the renormalized action \tilde{S}_0 , then

$$\begin{aligned} Z[\bar{\eta}, \eta, J] &\rightarrow \tilde{Z}[\bar{\eta}, \eta, J] & , & \quad G[\dots] \rightarrow \tilde{G}[\bar{\eta}, \eta, J] \\ \Gamma[\bar{\Psi}, \Psi, A] &\rightarrow \tilde{\Gamma}[\bar{\Psi}, \Psi, A] & , & \quad S^f(p) \rightarrow \tilde{S}^f(p) \\ D^{\mu\nu}(p) &\rightarrow \tilde{D}^{\mu\nu}(p) & , & \quad \underline{\text{etc.}} \end{aligned}$$

Gauge invariance now \Rightarrow relations between renormalized n -point Green's functions i.e., WTI still hold for renormalized quantities

Clearly then e.g. $k_\mu \tilde{\Pi}^{\mu\nu}(k) = 0$

$$k_\mu \tilde{\Gamma}^{f\mu}(p+k, p) = (\tilde{S}^f)^{-1}(p+k) - (\tilde{S}^f)^{-1}(p)$$

The second of these also $\Rightarrow [Z_1 = Z_2]!$
(not true for QCD, see later) \curvearrowright

→ The choice of renormalization point " μ " by definition must have no effect on physical observables.

In QED the "on-shell" renormalizⁿ point is merely the typical choice.

The unrenormalized quantities depend only on the regularizⁿ parameter (Λ), i.e., $e_0^f(\Lambda)$, $m_0^f(\Lambda)$, $S_0^f(\Lambda)$.

Can have:

momentum cut-off
dimensional regularization
etc.

$$\Lambda = \Lambda_{UV}$$
$$\Lambda = \frac{1}{\epsilon} \quad (D=4-2\epsilon)$$

The renormalization constants depend on μ and Λ
i.e., $Z_1(\mu, \Lambda)$, $Z_2(\mu, \Lambda)$, $Z_3(\mu, \Lambda)$

The renormalization group equations determine
how to vary μ while keeping Λ and
 $e_0^f(\Lambda)$, $m_0^f(\Lambda)$, $g_0(\Lambda)$ fixed.
 \Rightarrow physical quantities also fixed.

e.g., consider the renormalized fermion propagator
 $\tilde{S}^f(p)$.

By Lorentz invariance can define (drop flavor index "f" now)

$$\tilde{S}(p) \equiv \frac{1}{\tilde{A}(p^2) \not{p} - \tilde{B}(p^2)} \equiv \frac{1}{\tilde{A}(p^2)} \frac{1}{\not{p} - \tilde{M}(p^2)}, \quad \tilde{M} \equiv \frac{\tilde{B}}{\tilde{A}}$$

By definition, at the renormalization point μ
 $\tilde{A}(\mu^2) = 1$ and $\tilde{B}(\mu^2) = \tilde{M}(\mu^2) \equiv m(\mu)$.

In general $\tilde{A}(p^2)$, $\tilde{B}(p^2)$, $m(\mu)$ vary with μ
(i.e., $m(\mu) \neq$ physical mass).

m_{phys} is pole in \tilde{S} , i.e., solⁿ of $m_{\text{phys}}^2 = M^2(m_{\text{phys}}^2)$
 $\Rightarrow m_{\text{phys}} = m(\mu)$ when μ^2 set to m_{phys}^2 (on-shell renormⁿ)

Reminder of why QED is a relatively "clean" QFT to study using DSE's:

* All quantities understood as renormalized (drop "tildes" notation).
The WTI for the vertex

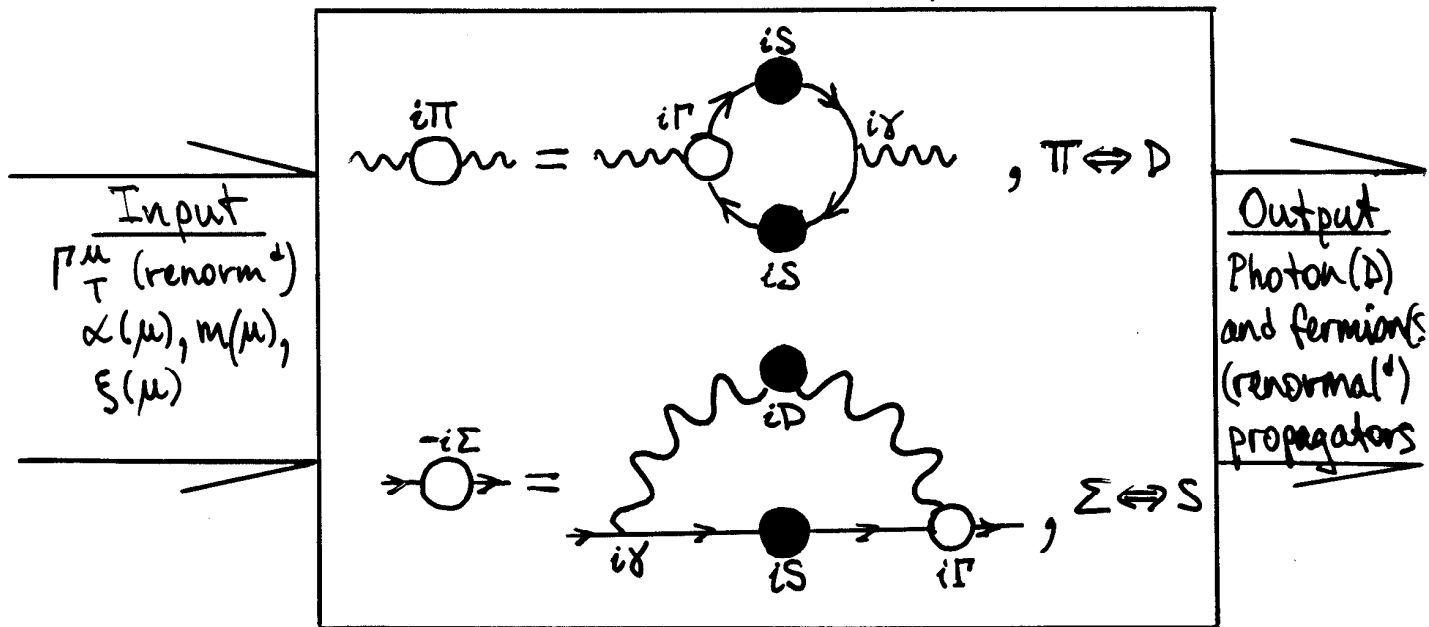
$$\text{[i.e., } k_\mu \Gamma^\mu(p+k, p) = S^{-1}(p+k) - S^{-1}(p) \text{]}$$

tells us that only the transverse part of vertex is unknown, i.e., Γ_T^μ s.t. $k_\mu \Gamma_T^\mu = 0$.

If we know $\Gamma_T^\mu \Rightarrow$ know all of $\Gamma^\mu(p+k, p)$

\Rightarrow fermion and photon propagators are fully determined !!

i.e., DSE's for $D^{\mu\nu}$ and S depend only on each other and Γ^μ .



A "state-of-the-art" study for quenched QED₄ in arbitrary covariant gauge:

From now on drop the " \sim " notation for renormalized quantities, (we will understand all quantities as renormalized).

→ Work in Euclid. space (i.e., as for LGT) for numerical tractability

→ Work in "quenched" approxⁿ i.e., $\begin{cases} Z_3(\mu, \Lambda) = 1 \\ \Pi^{\mu\nu} \rightarrow 0 \end{cases}$

$$D^{\mu\nu}(k) \leadsto D_0^{\mu\nu}(k) = \left\{ \frac{(-g^{\mu\nu} + \frac{k^\mu k^\nu}{k^2})}{k^2} - \int \frac{k^\mu k^\nu}{k^2} \right\}$$

→ Use WTI for Γ^μ and also requirements of multiplicative renormalizability, CPT properties etc to restrict the form of this. "State of art" vertex is due to Curtis + Pennington.

⇒ class of possible fermion-photon proper vertices Γ^μ remain.

* Current efforts to further constrain Γ_T^μ .

→ Can now study numerically DCSB and structure of fermion propagator by solving fermion DSE. (Numerically iterate integral equⁿ).

The Curtis-Pennington Vertex:

(see eq C+P, PRD 48, 4433 (1993))

- bare vertex: $\Gamma^\mu(p', p) \rightarrow \gamma^\mu$

- Ball-Chiu vertex: (satisfies Ward and WTI)

$$\Gamma_{BC}^\mu(p', p) \equiv \frac{[A(p'^2) + A(p^2)]}{2} \gamma^\mu + \frac{(p'+p)^\mu}{p'^2 - p^2} \left\{ [A(p'^2) - A(p^2)] \frac{p'+p}{2} - [B(p'^2) - B(p^2)] \right\}$$

- Curtis-Pennington vertex: (satisfies Ward and WTI and reproduces correct UV behaviour)

$$\Gamma^\mu(p', p) \rightarrow \Gamma_{CP}^\mu(p', p) \equiv \Gamma_{BC}^\mu(p', p) + \left\{ \left[\frac{(p'^2 - p^2) + [M^2(p'^2) + M^2(p^2)]^2}{p'^2 + p^2} \right]^{-1} \frac{1}{2} [A(p'^2) - A(p^2)] \times [\gamma^\mu (p'^2 - p^2) - (p'+p)^\mu (p'^2 - p^2)] \right\}$$

Of course, want to study various ansätze for transverse vertex and further constrain its form.

But as we will see some important observations and results follow indep of detailed choice of this.

Most general possible vertex:

The most general possible vertex can be specified in terms of 8 transverse functions (τ_1, \dots, τ_8) .

$$\Gamma^\mu(k, p) = \Gamma_{BC}^\mu(k, p) + \Gamma_T^\mu(k, p)$$

where we define $q^\mu \equiv k^\mu - p^\mu$. Note $q_\mu \Gamma_T^\mu = 0$.

The Ball-Chiu vertex is defined as

$$\Gamma_{BC}^\mu(k, p) \equiv \frac{[A(k^2) + A(p^2)]}{2} \gamma^\mu + \frac{(k+p)^\mu}{(k^2 - p^2)} \left\{ \begin{array}{l} [A(k^2) - A(p^2)] \frac{k+p}{2} \\ - [B(k^2) - B(p^2)] \end{array} \right\}$$

and we define

$$\Gamma_T^\mu(k, p) \equiv \sum_{i=1}^8 \tau_i(k^2, p^2, q^2) T_i^\mu(k, p),$$

where the 8 linearly independent transverse vectors form a basis for Γ_T^μ and are given by:

$$T_1^\mu(k, p) \equiv p^\mu(k \cdot q) - k^\mu(p \cdot q)$$

$$T_2^\mu(k, p) \equiv T_1^\mu(k+p)$$

$$T_3^\mu(k, p) \equiv q^2 \gamma^\mu - q^\mu q^\nu$$

$$T_4^\mu(k, p) \equiv q^2 [\gamma^\mu (k+p) - k^\mu - p^\mu] - 2(k-p)^\mu \sigma_{\lambda\nu} k^\lambda p^\nu$$

$$T_5^\mu(k, p) \equiv -\sigma^{\mu\nu} q_\nu$$

$$T_6^\mu(k, p) \equiv \gamma^\mu (k^2 - p^2) - (k+p)^\mu (k-p)$$

$$T_7^\mu(k, p) \equiv -\frac{1}{2}(k^2 - p^2) [\gamma^\mu (k+p) - k^\mu - p^\mu] + (k+p)^\mu \sigma_{\lambda\nu} k^\lambda p^\nu$$

$$T_8^\mu(k, p) \equiv \gamma^\mu \sigma_{\lambda\nu} k^\lambda p^\nu - k^\mu \not{p} + p^\mu \not{k}$$

Numerical subtractive renormalization

procedure: $\left[\text{Recall defns } \begin{aligned} S(p)^{-1} &= A(p^2) \not{p} - B(p^2) \\ &= \not{p} - m(\mu) - \tilde{\Sigma}(p) \end{aligned} \right]$

① Choose $\mu, g(\mu), \alpha(\mu), m(\mu)$, and regularization parameter Λ

② Make initial guess for $A(p^2)$ and $B(p^2)$ and also for $z_1 = z_2$

③ Calculate

$$-i \Sigma' = z_1 4\pi\alpha \int \frac{d^4 \ell}{(2\pi)^4} \gamma S D \Gamma$$

and hence find Σ'_S and Σ'_D
and then

$$\tilde{\Sigma}_{\{S, D\}}(\mu; p^2) \equiv \Sigma'_{\{S, D\}}(\mu, \Lambda; p^2) - \Sigma'_{\{S, D\}}(\mu, \Lambda; \mu^2)$$

which ensures correct renormalization pt BC's
(i.e., $\tilde{\Sigma}_S(p^2 = \mu^2) = 0, \tilde{\Sigma}_D(p^2 = \mu^2) = 0$).

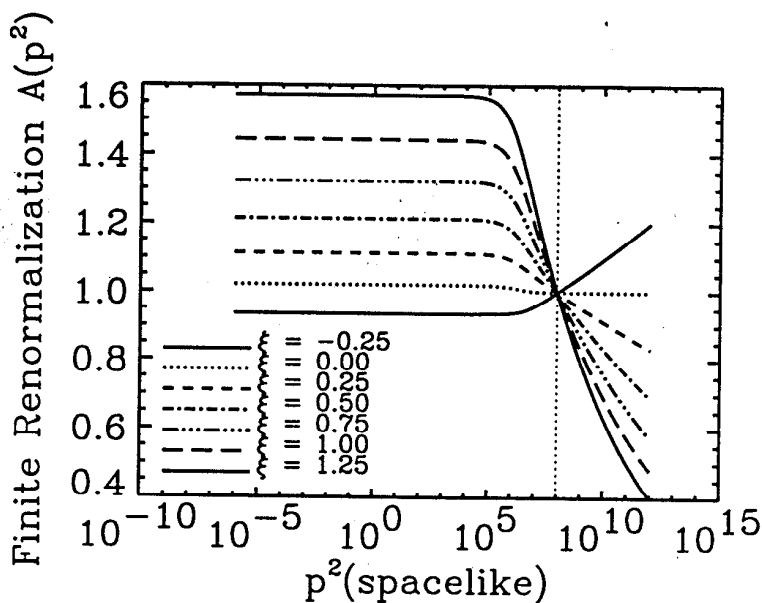
④ Then have

$$\begin{cases} A(p^2) \equiv 1 - \tilde{\Sigma}_D(\mu; p^2) \\ B(p^2) \equiv m(\mu) + \tilde{\Sigma}_S(\mu; p^2) \\ z_1(\mu; \Lambda) = z_2(\mu; \Lambda) \equiv 1 + \Sigma'_D(\mu, \Lambda; \mu^2) \\ m_0(\Lambda) \equiv [m(\mu) - \Sigma'_S(\mu, \Lambda; \mu^2)] / z_2(\mu, \Lambda) \end{cases}$$

Cycle until convergence. (Typically 20-50 cycles for 10^{-4} relative error).
i.e., wait until A and B no longer change.

Results with an ultraviolet cutoff
regulator, $\Lambda \equiv \Lambda_{uv}$.

FIGURES



Recall

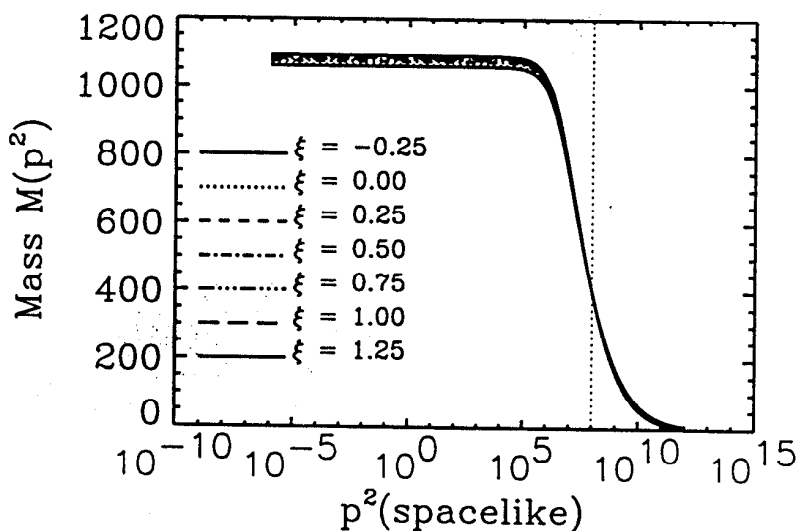
$$S^{-1}(p) \equiv A(p^2)\not{p} - B(p^2)$$

$$\equiv Z(p^2)^{-1} [\not{p} - M(p^2)]$$

$$\equiv \not{p} - m(\mu) - \tilde{\Sigma}(p)$$

i.e. $M(p^2) = \frac{B(p^2)}{A(p^2)}$

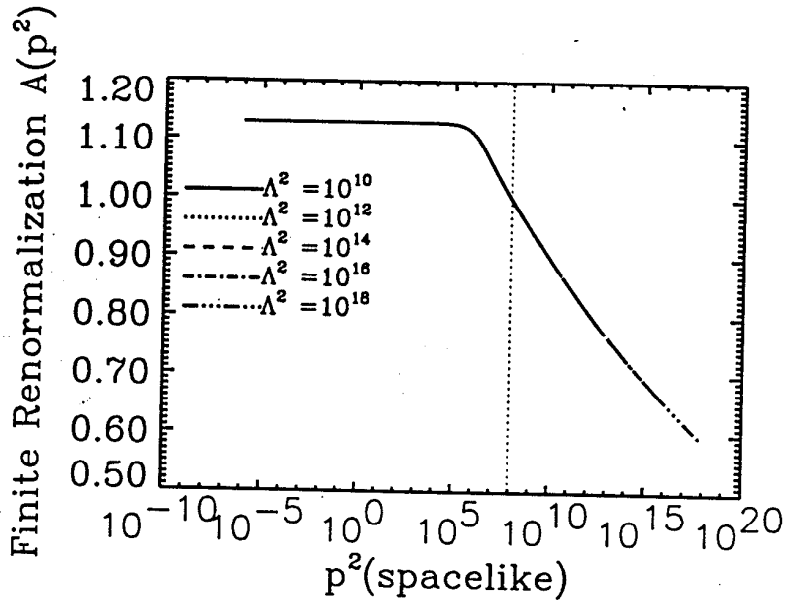
$$Z(p^2) = \frac{1}{A(p^2)}$$



Only the physical mass (m_{phys}) and the bare mass should be strictly gauge invariant.

FIG. 1. The finite renormalization $A(p^2)$ and the mass function $M(p^2)$ are shown for various gauge parameters ξ . These results have coupling $\alpha = 1.00$, renormalization point $\mu^2 = 10^8$, and renormalized mass $m(\mu) = 400$. In the low p^2 region the larger gauge parameter has the larger value of $M(p^2)$.

CP vertex (with gauge-covariance correction)



Continuum
limit of the
solutions exists!

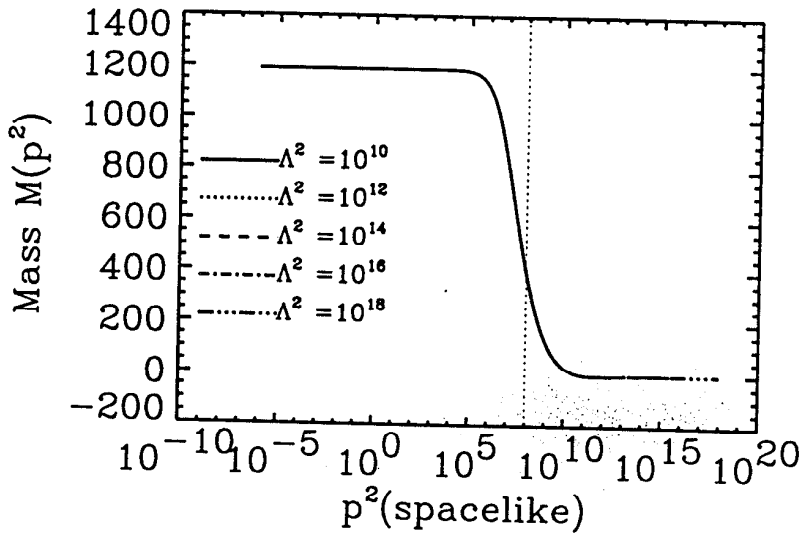
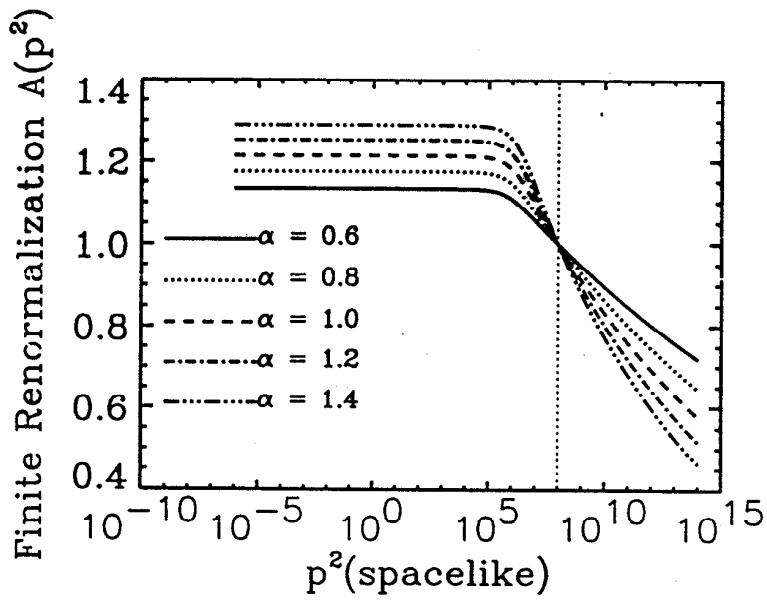


FIG. 2. The finite renormalization $A(p^2)$ and the mass function $M(p^2)$ are shown for various choices of the regularization parameter (i.e., ultraviolet cut-off) Λ . These results have coupling $\alpha = 1.15$, renormalization point $\mu^2 = 10^8$, renormalized mass $m(\mu) = 400$, and gauge parameter $\xi = 0.25$. The stability of the subtractive renormalization procedure is apparent.



Critical coupling
is $\alpha_c \approx 0.95$

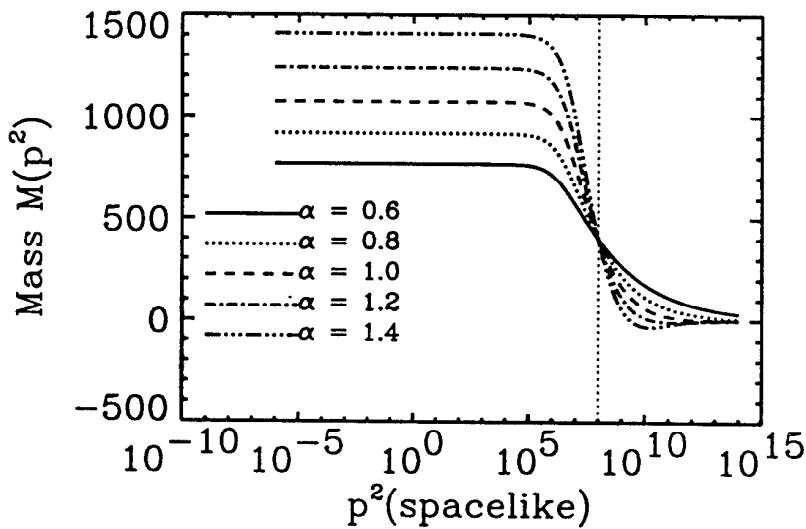
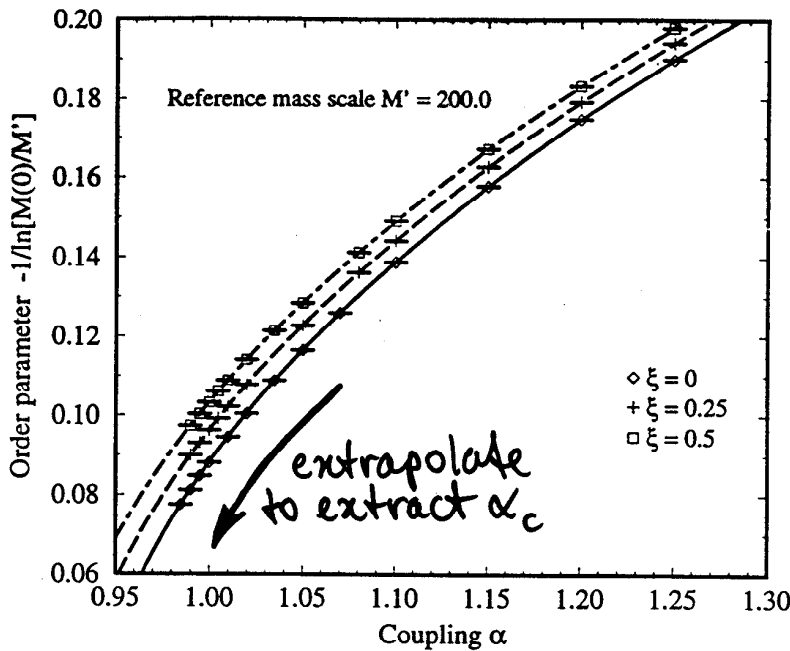


FIG. 3. The finite renormalization $A(p^2)$ and the mass function $M(p^2)$ are shown for various choices of the coupling strength α . These results have renormalization point $\mu^2 = 10^8$, renormalized mass $m(\mu) = 400$, and gauge parameter $\xi = 0.50$.

Critical Curves for gauges $\xi = 0, 0.25, 0.5$



⇒ Critical coupling is $\alpha_c \approx 0.95$
Slight gauge dependence.

FIG. 4. The critical curves for three choices of gauge parameter showing the existence of residual gauge-dependence in the Curtis-Pennington vertex. All solutions were renormalized at the chiral limit, i.e., $m(\mu) = 0$, with the renormalization point $\mu^2 = 10^4$. The order parameter is evaluated using an arbitrary reference mass scale choice of $M' = 200.0$. Diamonds (\diamond) connected by the solid smooth curve, are order parameter values for the Landau gauge; pluses (+) connected by the dashed smooth curve, are values for $\xi = 0.25$; and boxes (\square) connected by the dot-dashed smooth curve, are values for $\xi = 0.5$.

Critical coupling (i.e., onset of dynamical mass generation) should be independent of gauge.

⇒ gauge-dependent α_c due to UV cutoff regulator (Λ) and/or non-ideal choice of transverse vertex (Γ_T^μ).

The WTI satisfied by Γ^μ is a necessary but not sufficient condition for gauge covariance of the fermion propagator.

Renormalization Point Transformations:

Multiplicative renormalizability \Rightarrow

$$S(p) \propto \frac{1}{Z_2(\mu, \Lambda)}, \quad D(p) \propto \xi(\mu) \propto \frac{1}{Z_3(\mu, \Lambda)}$$
$$e(\mu) \propto \frac{Z_2(\mu, \Lambda) \sqrt{Z_3(\mu, \Lambda)}}{Z_1(\mu, \Lambda)}, \quad e(\mu) \Gamma^\mu \propto \frac{Z_2(\mu, \Lambda) \sqrt{Z_3(\mu, \Lambda)}}{\sqrt{Z_3(\mu, \Lambda)}} \quad (\text{since } Z_1 = Z_2)$$

In quenched QED₄ we have $e(\mu) = e$, $Z_3 = 1$
and so

$$S(p) \propto \frac{1}{Z_2(\mu, \Lambda)} \quad \Gamma^\mu(p', p) \propto Z_2(\mu, \Lambda).$$

Recall that $S(p) \equiv \frac{1}{A(p^2) \not{p} - B(p^2)} \equiv \frac{1}{A(p^2) [\not{p} - M(p^2)]}$.

Hence, under a renormalizⁿ point transformⁿ
we see that

$$A(p^2) \propto Z_2(\mu, \Lambda), \quad B(p^2) \propto Z_2(\mu, \Lambda), \quad \Gamma^\nu(p', p) \propto Z_2(\mu, \Lambda)$$

Conclusions:

① Multiplicative renormalizⁿ requires that $\Gamma^\nu(p', p)$ must be chosen to scale
st. if $A \rightarrow cA$, $B \rightarrow cB$
then $\Gamma^\nu \rightarrow c \Gamma^\nu$ for any constant "c"

② $A(p^2)/Z_2(\mu, \Lambda)$ and $M(p^2)$ are
renormalⁿ point independent.

Verify numerically. (Our Γ_{CP}^ν scales appropriately).

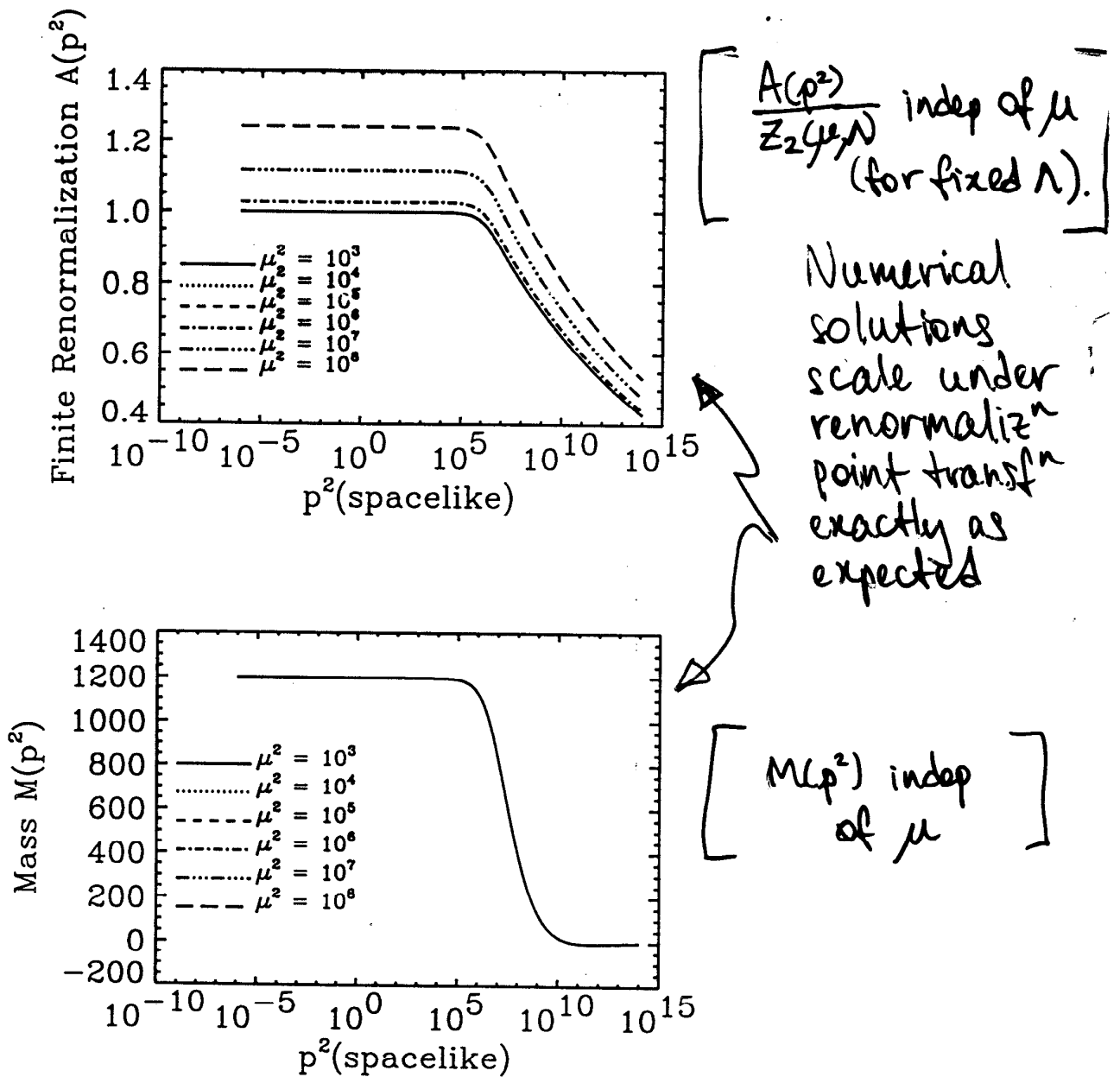


FIG. 5. The finite renormalization $A(p^2)$ and the mass function $M(p^2)$ are shown for various choices of renormalization point. These results have coupling strength $\alpha = 1.15$ and gauge parameter $\xi = 0.50$. Each of these results corresponds to $M(p^2) = 400$ at $p^2 = 10^8$. Hence, $M(p^2)$ is renormalization point independent and $A(p^2)$ varies as described in Eq. (30).

CP vertex (with gauge covariance correction)

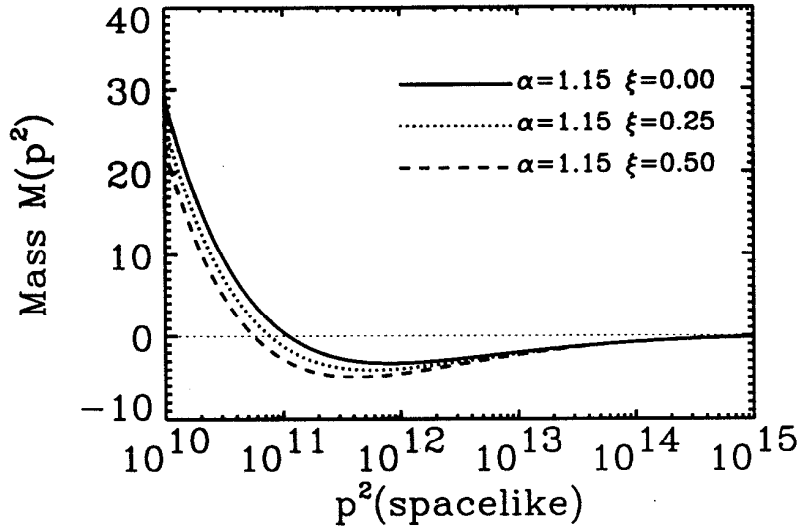


FIG. 8. Detail of the node in the mass function $M(p^2)$ for various gauge choices. These results have coupling strength $\alpha = 1.15$, renormalization point $\mu^2 = 10^8$, and renormalized mass $m(\mu) = 400$.

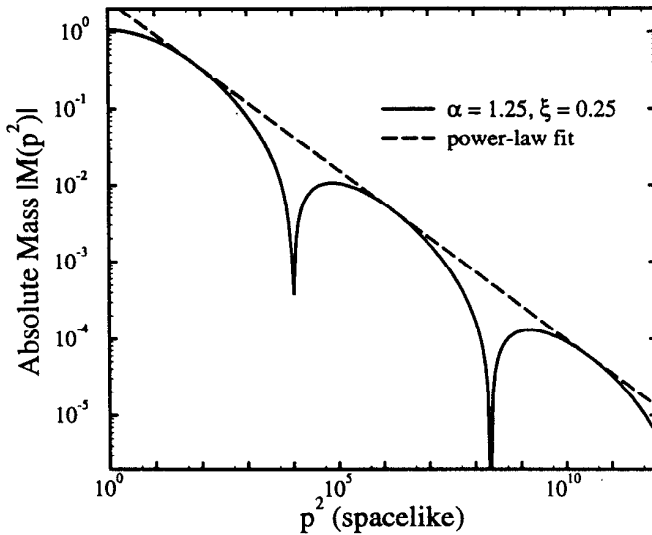


FIG. 9. Absolute value of the dynamical mass, showing damped oscillations periodic in $\ln(p^2)$. The solution shown has $\alpha = 1.25$, $\xi = 0.25$, and is renormalized with $\mu^2 = 10^4$, $m(\mu) = 0$. The power-law fit, which runs tangent to the dynamical mass curve, is $C(p^2/\mu^2)^{(\gamma_m/2)-1}$, with $C = 4.394 \times 10^{-2}$, $\gamma_m = 1.115$.

For supercritical α
 (i.e., Dynamical chiral
 symmetry breaking)
 and large enough
 UV cut-off (Λ)
 we always find decaying
 UV oscillations in
 the mass function!

Here $Z_m(\mu, \Lambda) \equiv \frac{m_0(\Lambda)}{m(\mu)}$

TABLES

TABLE I. Renormalization constant $Z_2(\mu, \Lambda)$, bare masses $m_0(\Lambda)$, and mass renormalization $Z_m(\mu, \Lambda)$, as a function of UV cutoff for $\alpha = 1.15$ in the Landau gauge ($\xi = 0$). All solutions are with renormalization point $\mu^2 = 1.00 \times 10^8$ and renormalized mass $m(\mu) = 400.0$

Λ^2	$Z_2(\mu, \Lambda)$	$m_0(\Lambda)$	$Z_m(\mu, \Lambda)$
1×10^8	0.9999135	2.306×10^2	5.765×10^{-1}
1×10^9	0.9998483	5.358×10^1	1.339×10^{-1}
1×10^{10}	0.9998468	4.443	1.111×10^{-2}
1×10^{11}	0.9998469	-3.932	-9.831×10^{-3}
1×10^{12}	0.9998469	-2.847	-7.117×10^{-3}
1×10^{13}	0.9998469	-1.182	-2.954×10^{-3}
1×10^{14}	0.9998469	-3.408×10^{-1}	-8.520×10^{-4}
1×10^{15}	0.9998469	-5.390×10^{-2}	-1.348×10^{-4}
1×10^{16}	0.9998469	1.043×10^{-2}	2.607×10^{-5}
1×10^{17}	0.9998469	1.276×10^{-2}	3.191×10^{-5}
1×10^{18}	0.9998469	6.171×10^{-3}	1.543×10^{-5}
1×10^{19}	0.9998469	2.042×10^{-3}	5.105×10^{-6}

TABLE II. Renormalization constant $Z_2(\mu, \Lambda)$, bare masses $m_0(\Lambda)$, and mass renormalization $Z_m(\mu, \Lambda)$, as a function of UV cutoff for $\alpha = 1.15$ in the gauge with $\xi = 0.25$. All solutions are with renormalization point $\mu^2 = 1.00 \times 10^8$ and renormalized mass $m(\mu) = 400.0$

Λ^2	$Z_2(\mu, \Lambda)$	$m_0(\Lambda)$	$Z_m(\mu, \Lambda)$
1×10^8	0.999943	2.239×10^2	5.598×10^{-1}
1×10^9	0.9486	4.918×10^1	1.229×10^{-1}
1×10^{10}	0.8999	2.034	5.085×10^{-3}
1×10^{11}	0.8537	-4.898	-1.225×10^{-2}
1×10^{12}	0.8099	-3.102	-7.756×10^{-3}
1×10^{13}	0.7683	-1.193	-2.981×10^{-3}
1×10^{14}	0.7289	-3.059×10^{-1}	-7.647×10^{-4}
1×10^{15}	0.6915	-2.886×10^{-2}	-7.214×10^{-5}
1×10^{16}	0.6560	2.145×10^{-2}	5.362×10^{-5}
1×10^{17}	0.6224	1.609×10^{-2}	4.023×10^{-5}
1×10^{18}	0.5904	6.679×10^{-3}	1.670×10^{-5}

Note: $m_0(\Lambda)$ oscillates and decreases as $\Lambda \rightarrow \infty$

Renormalizⁿ constants stay finite as $\Lambda \rightarrow \infty$!
(Purely nonperturbative result.)

TABLE III. Renormalization constant $Z_2(\mu, \Lambda)$, bare masses $m_0(\Lambda)$, and mass renormalization $Z_m(\mu, \Lambda)$, as a function of UV cutoff for $\alpha = 1.15$ in the gauge with $\xi = 0.5$. All solutions are with renormalization point $\mu^2 = 1.00 \times 10^8$ and renormalized mass $m(\mu) = 400.0$

Λ^2	$Z_2(\mu, \Lambda)$	$m_0(\Lambda)$	$Z_m(\mu, \Lambda)$
1×10^8	0.99997	2.176×10^2	5.441×10^{-1}
1×10^9	0.8999	4.513×10^1	1.128×10^{-1}
1×10^{10}	0.8099	-1.455×10^{-1}	-3.638×10^{-4}
1×10^{11}	0.7289	-5.736	-1.434×10^{-2}
1×10^{12}	0.6560	-3.299	-8.248×10^{-3}
1×10^{13}	0.5904	-1.181	-2.954×10^{-3}
1×10^{14}	0.5314	-2.653×10^{-1}	-6.632×10^{-4}
1×10^{15}	0.4783	-3.676×10^{-3}	-9.190×10^{-6}
1×10^{16}	0.4304	3.151×10^{-2}	7.877×10^{-5}
1×10^{17}	0.3874	1.870×10^{-2}	4.674×10^{-5}

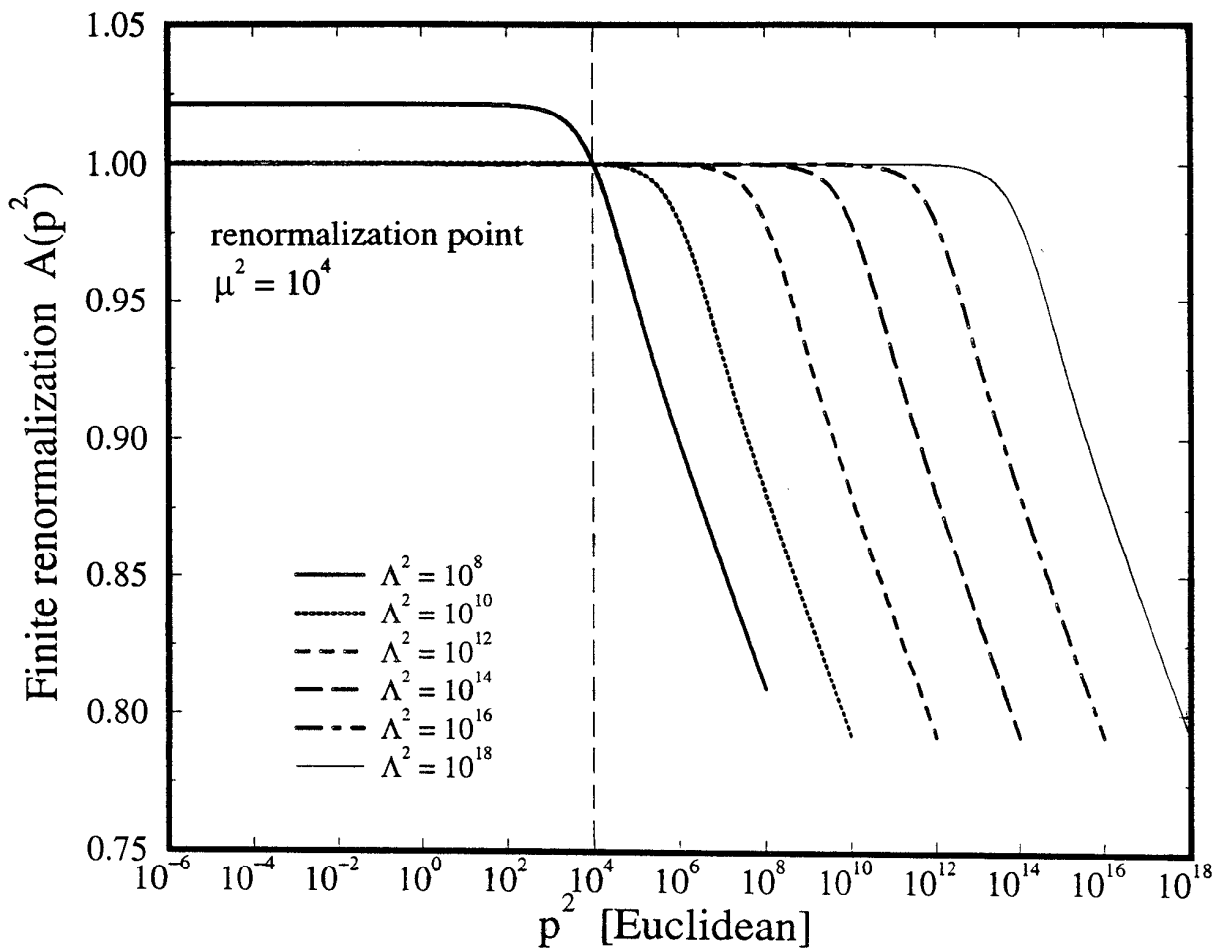
TABLE IV. Critical parameters for three choices of gauge, $\xi = 0, 0.25$, and 0.50 . These are extracted from nonlinear fits to the data in Fig. 4, using the form in Eq. (32).

Parameter	Landau ($\xi = 0$)	$\xi = 0.25$	$\xi = 0.5$
c	$2.877 \pm .027$	$2.858 \pm .043$	$2.851 \pm .055$
α_c	$0.93307 \pm .00023$	$0.92076 \pm .00048$	$0.90946 \pm .00071$
β	$0.512 \pm .003$	$0.514 \pm .005$	$0.516 \pm .007$
M	154.3 ± 5.2	148.5 ± 7.7	145.4 ± 9.4
χ^2/DOF	0.0959	.0388	.0211

small gauge-dependence of α_c ,
(UV regulator).

Note: For -ve gauge parameter $Z_2(\mu, \Lambda)$ does increase and diverge with Λ .
But of course $A(p^2)$ and $M(p^2)$ stay finite.

$A(p^2)$ for several UV cutoffs



Numerical verification of scaling behaviour. ✓

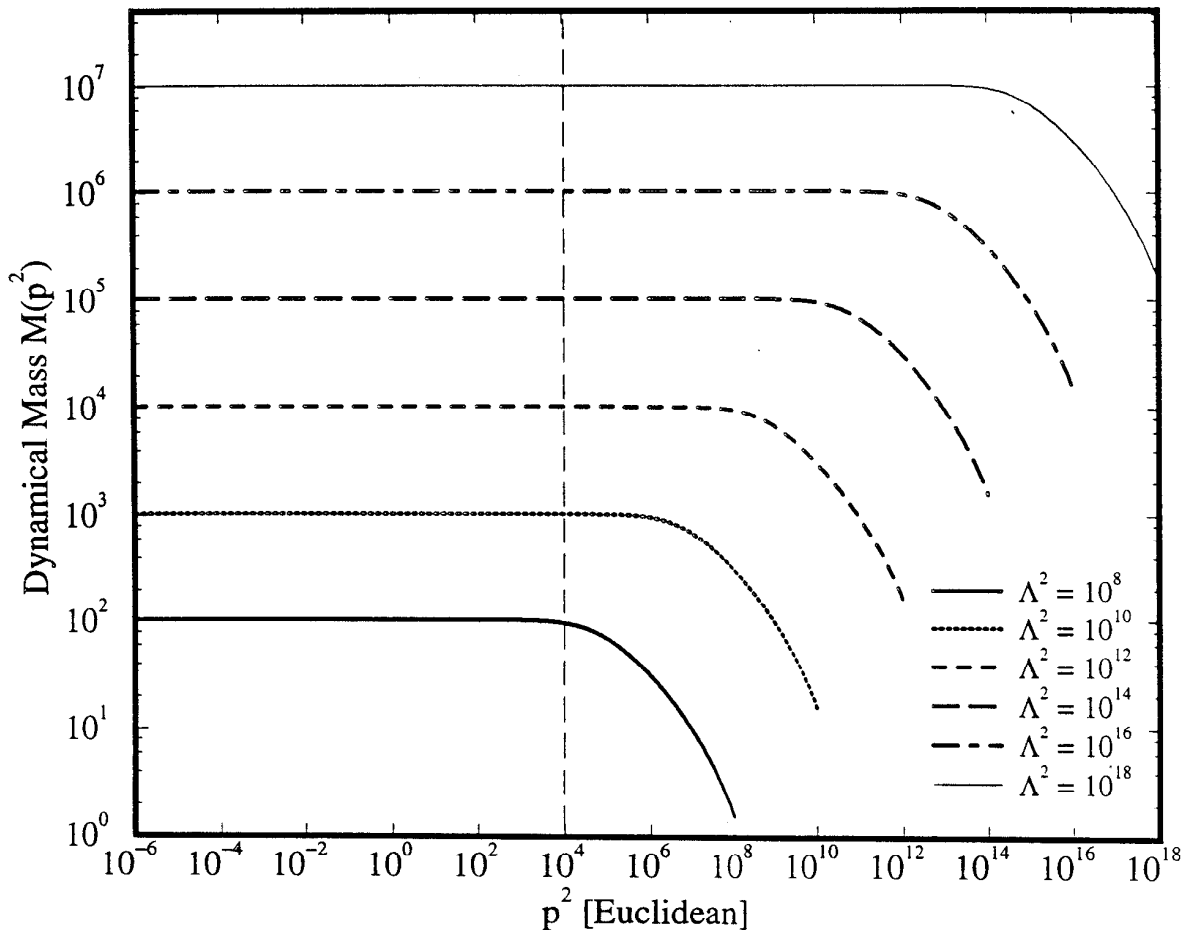
All curves correspond to same $\hat{A}(\hat{p}^2) \equiv A(p^2) / Z_2(\mu, \Lambda)$

Clearly, the limit $\Lambda \rightarrow \infty$ with $m_0(\Lambda) = 0$ exists for $A(p^2)$ for all α

i.e.

$A(p^2) \rightarrow 1$ for all p^2 and any α in the continuum chiral limit.

$M(p^2)$ for several UV cutoffs



Numerical verification of scaling behaviour. ✓
 All curves correspond to same $\hat{M}(\hat{p}^2)$.

No chiral limit in presence of DCSB
 (i.e., above critical coupling; $\alpha > \alpha_c$).

Note: Below critical coupling ($\alpha < \alpha_c$) the
 $\Lambda \rightarrow \infty$ with $m_0(\Lambda) = 0$ limit does exist
 i.e. solution for continuum chiral limit
 is $M(p^2) = 0$, $A(p^2) = 1$ for all p^2 .

Simple proof of absence of finite chiral limit in renormalized quenched DSE studies of QED₄ (for $\alpha > \alpha_c$; supercritical coupling):

- (i) Recall that $A(p^2)/Z_2(\mu, \Lambda)$ and $M(p^2)$ are renorm^l point (μ) independent.
- (ii) Define dimensionless functions in terms of dimensionless variables ($\hat{\mu} \equiv \mu/\Lambda$, $\hat{p}^2 \equiv p^2/\Lambda^2$)
 i.e. $\hat{A}(\hat{p}^2) \equiv \frac{A(p^2)}{Z_2(\mu, \Lambda)}$, $\hat{M}(\hat{p}^2) \equiv \frac{M(p^2)}{\Lambda}$

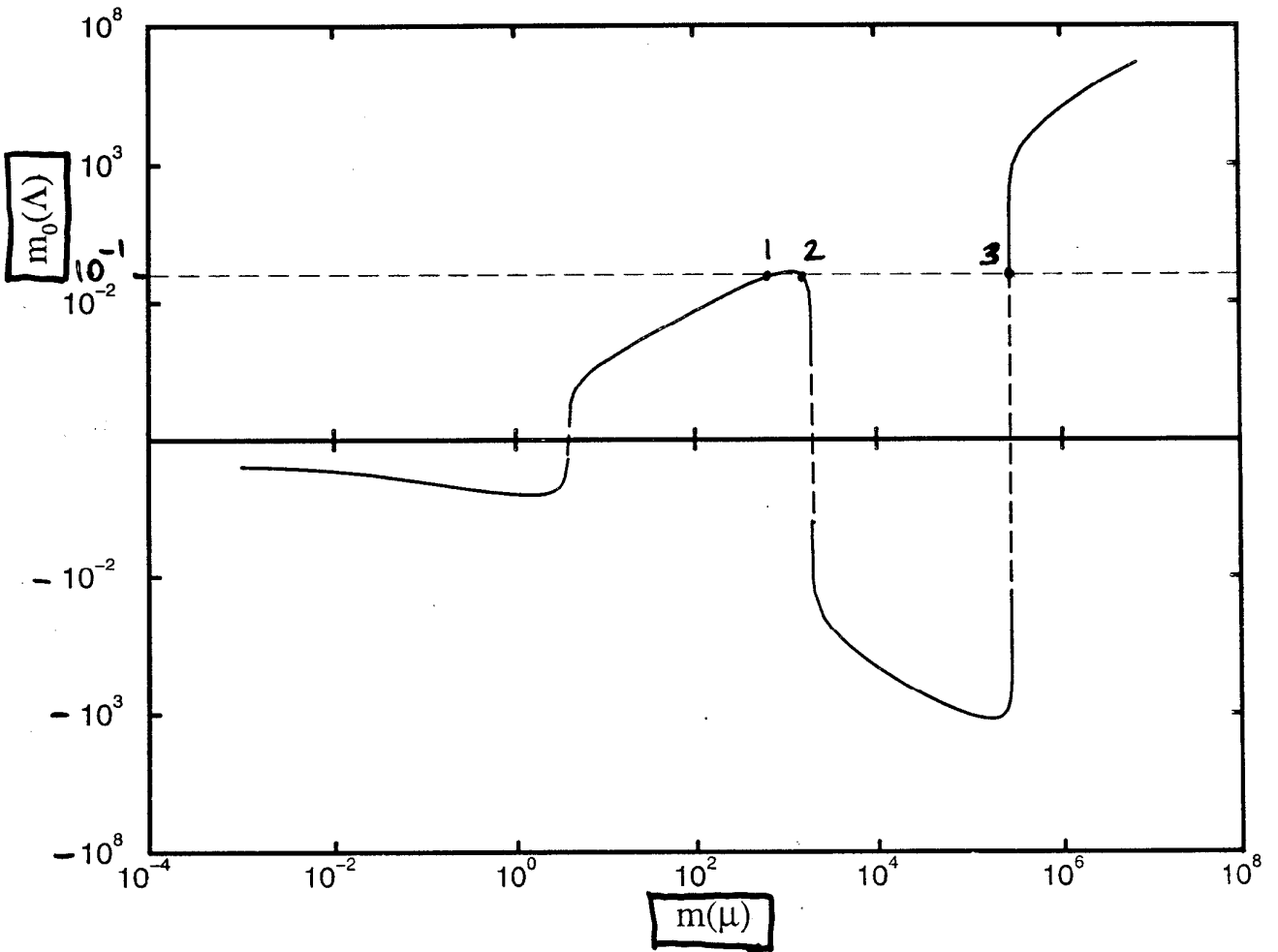
- (iii) The new functions $\hat{A}(\hat{p}^2)$ and $\hat{M}(\hat{p}^2)$ can only depend on $\hat{\mu}$, \hat{p}^2 , α , $m_0(\Lambda)/\Lambda$.

But they must be indep of $\hat{\mu}$ and if $m_0(\Lambda) = 0$ then they can only depend on \hat{p}^2 and α .

- (iv) So if zero bare mass ($m_0(\Lambda) = 0$), then dimensionless $\hat{M}(\hat{p}^2)$ depends only on α and \hat{p}^2 .
 \Rightarrow above critical coupling ($\alpha > \alpha_c$) where $\hat{M}(\hat{p}^2) \neq 0$, then $M(p^2) = \Lambda \hat{M}(\hat{p}^2)$ diverges as $\Lambda \rightarrow \infty$.

Conclusion: Above critical coupling ($\alpha > \alpha_c$) if $M(p^2) \neq 0$, then as $\Lambda \rightarrow \infty$ with $m_0(\Lambda) = 0$, $M(p^2)$ diverges \Rightarrow no (non-zero) chiral limit.

Figure 2



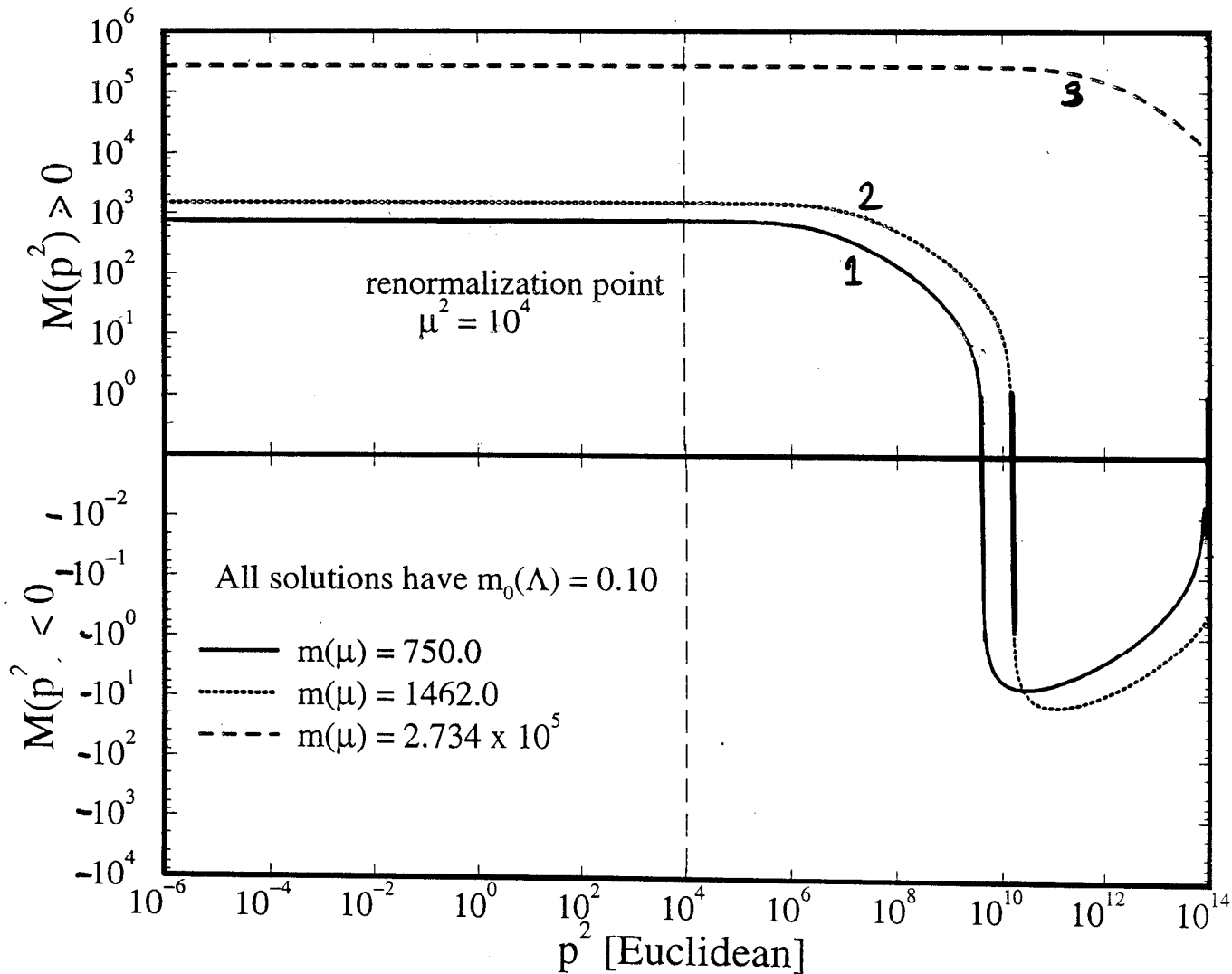
For given bare mass $m_0(\Lambda)$
there are multiple solutions!

$$\left[\begin{array}{l} \Lambda^2 = 10^{14} \\ \alpha = 1.25 \\ \mu^2 = 10^4 \end{array} \right]$$

e.g. three solⁿs for $m_0(\Lambda) = 0.1$

For given renormalized mass $m(\mu)$ there
is a unique solution!

Multiple solutions for a specified bare mass



The three solutions corresponding to the same bare mass $m_0(\Lambda) = 10^{-1} = 0.1$

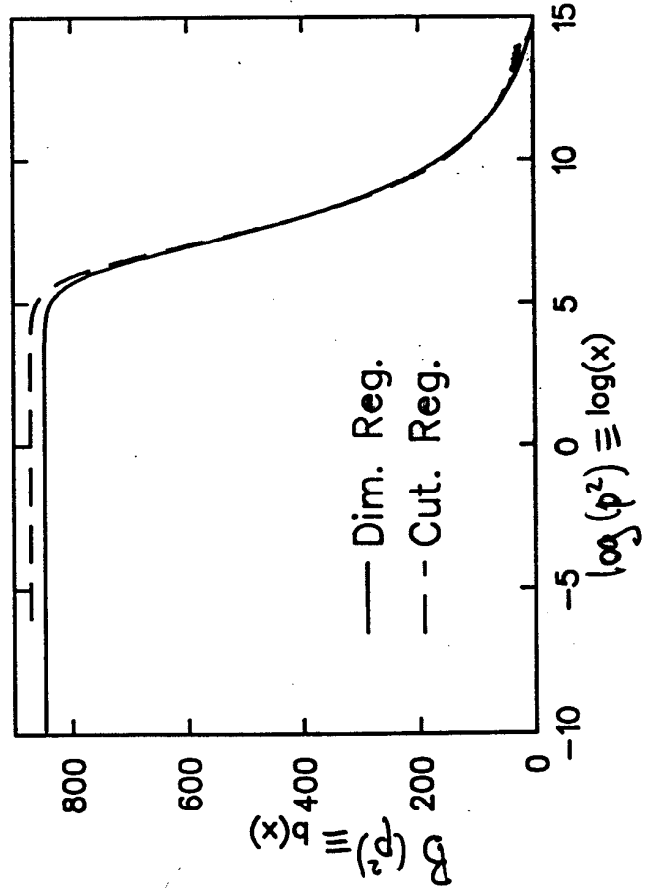
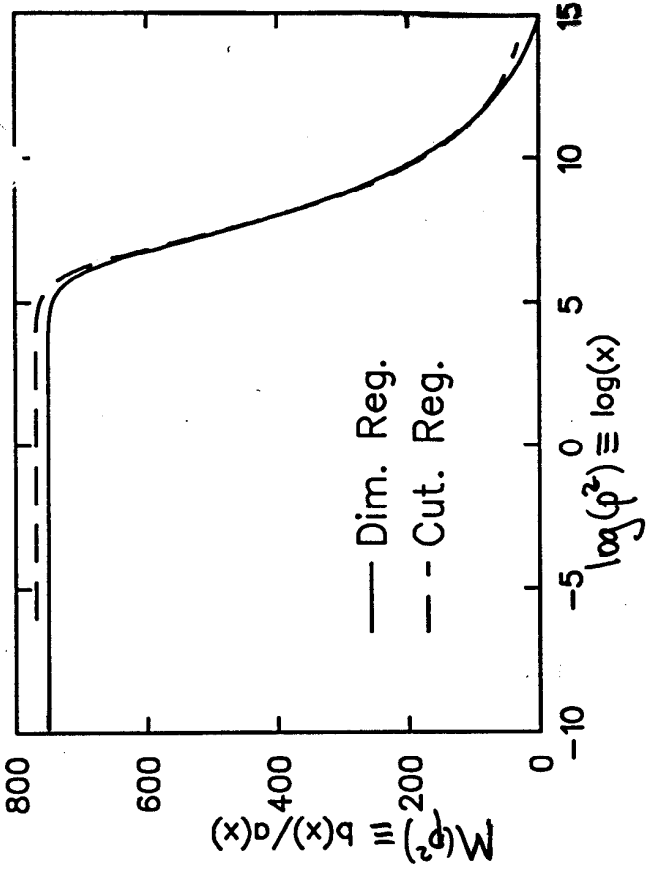
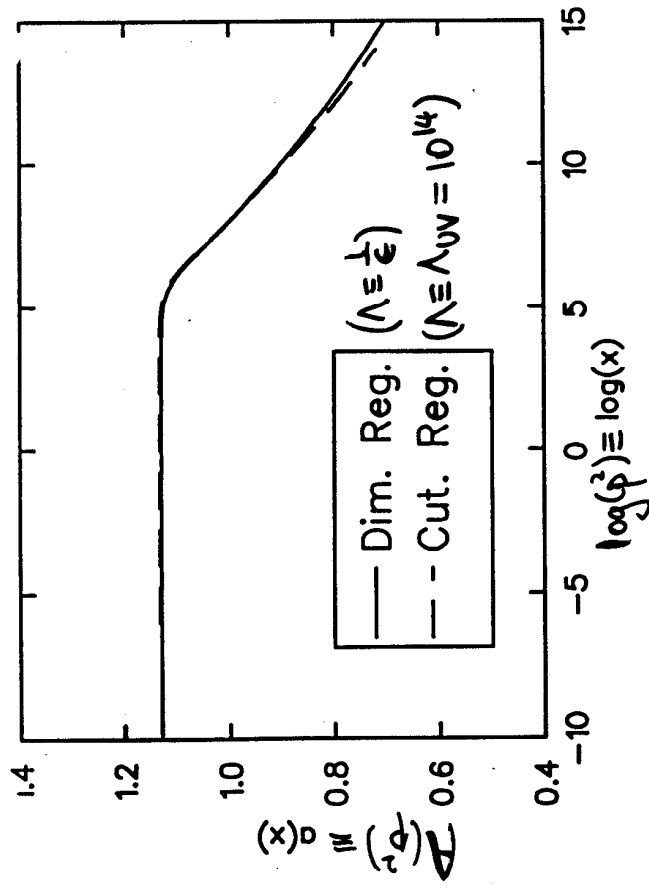
$$\left[\begin{array}{l} \Lambda^2 = 10^{14} \\ \alpha = 1.25 \\ \mu^2 = 10^4 \end{array} \right]$$

Note: As $\Lambda \rightarrow \infty$
the number of
solutions for same $m_0(\Lambda)$
 $\rightarrow \infty$!

Results from using dimensional regularization, $\Lambda \equiv \frac{1}{\epsilon}$, ($D = 4 - 2\epsilon$).

(Note: When using dim. reg. need to temporarily introduce another mass scale " ν " which becomes irrelevant) in the limit $\epsilon \rightarrow 0$.

- The following results are very new.
- All of the previous UV cut-off calculations are being re-done using dim. reg. instead.



Comparison of UV cutoff regularization to dimensional regularization (extrapolated to $\epsilon \rightarrow 0$)
 $\alpha = 0.6$

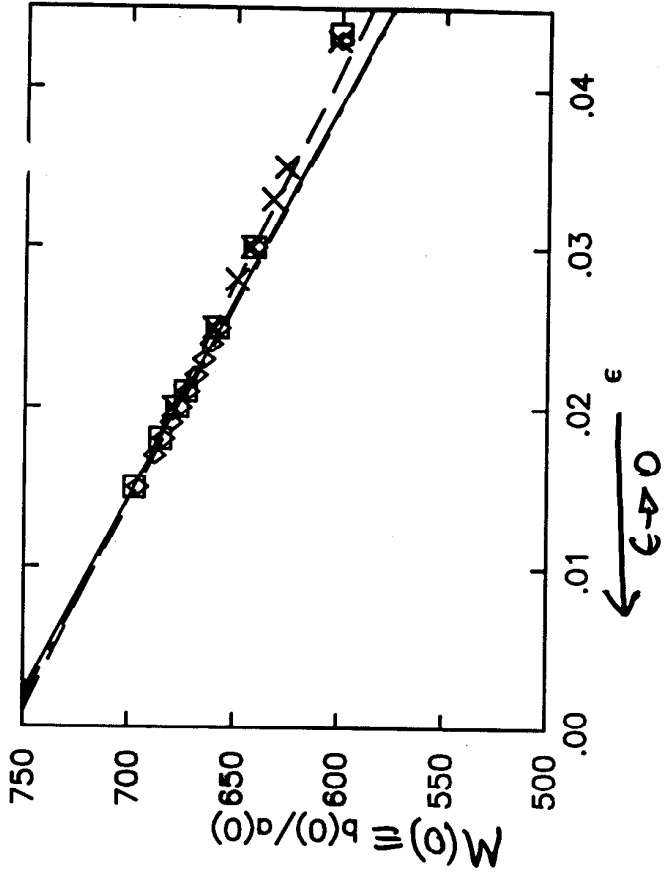
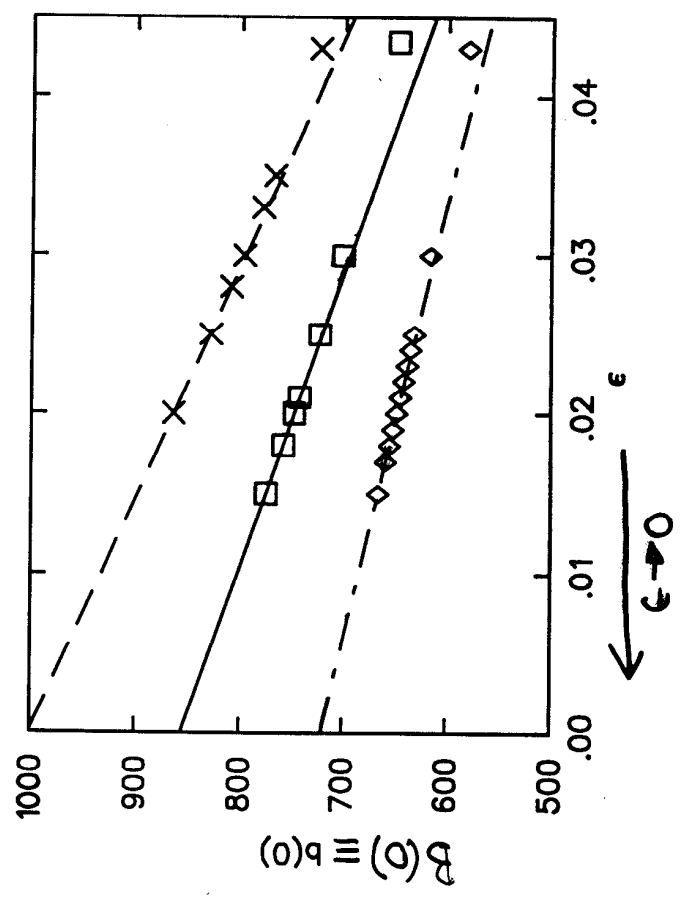
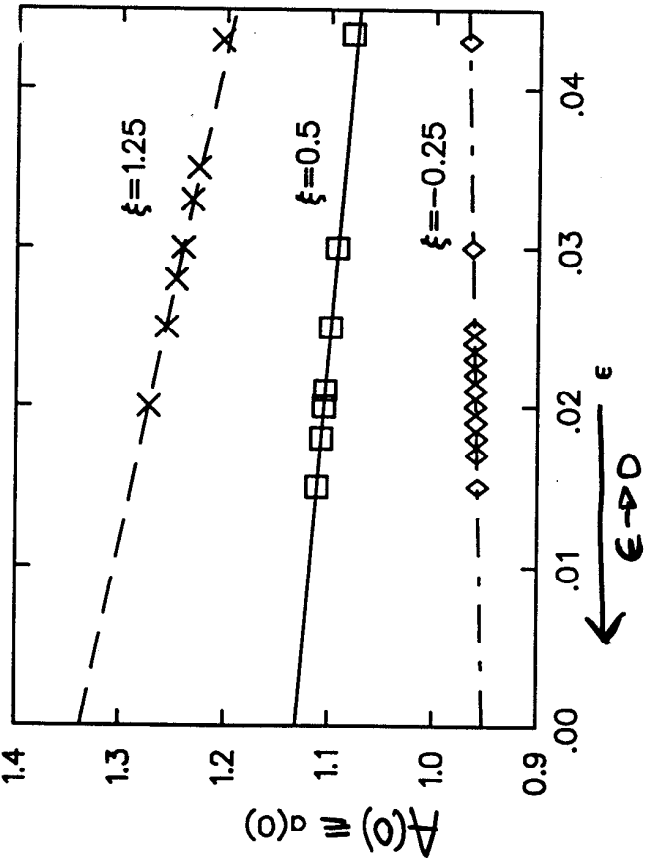
$\xi = 0.5$
 $M/\nu = 400$

$$(\mu^2/\nu^2 = 100000000) \Rightarrow \mu/\nu = 10^4$$

Set here, e.g., $\nu = 1 \text{ MeV}$.

Small difference between regularization schemes is expected, since e.g. UV cutoff violates gauge invariance whereas dim. reg. doesn't.

But otherwise results are very similar! The dim. reg. results are clearly the ones which are to be preferred.



Clearly the $\epsilon \rightarrow 0$ limit is very well behaved.

$\alpha = 0.6$
 $M/\nu = 400$
 $\mu/\nu = 10^4$

Set here, e.g., $\nu = 1 \text{ MeV}$.

Conclusions and Outlook:



Numerical implementation of nonperturbative renormalization works very well

- ⇒ can renormalize at any scale
- ⇒ renormalization group transformations explicitly tested and verified
- ⇒ solⁿ at one renormalizⁿ scale automatically gives solⁿs at all scales!

- Studies so far were for QED₄ with quenched photon, but generalization to other QFT's is straight forward
 - e.g. a) "Unquenched" QED₄ (i.e., $z_3 \neq 1$)
 - b) DSE-based studies of QCD
 - c) Improved vertex (?) } in progress
- Lattice studies of QFT always renormalize at zero momentum for external legs of n-point Green's fns.
 - * Can now directly compare to DSE's
- Successful implementation of dim. reg. is major advance.
- On general grounds quenched QED₄ has no finite chiral limit for $\alpha > \alpha_c$ in broken symmetry sector, (trivial solⁿ $M(p^2) = 0$ always exists in chiral limit) in unbroken symmetry sector.
- For CP vertex and $\alpha > \alpha_c$ the only finite solutions found were multiple solutions with UV oscillations, (and for $m_0(\lambda) = 0$ the trivial symmetric sector solution $M(p^2) = 0, \forall p^2$).
- Next major steps: (i) unquenching, (ii) improve vertex.